
Graph Unitary Message Passing

Haiquan Qiu¹ Yatao Bian² Quanming Yao¹

Abstract

Message passing mechanism contributes to the success of GNNs in various applications, but also brings the oversquashing problem. Recent works combat oversquashing by improving the graph spectrums with rewiring techniques, disrupting the structural bias in graphs, and having limited improvement on oversquashing in terms of oversquashing measure. Motivated by unitary RNN, we propose Graph Unitary Message Passing (GUMP) to alleviate oversquashing in GNNs by applying unitary adjacency matrix for message passing. To design GUMP, a transformation is first proposed to make general graphs have unitary adjacency matrix and keep its structural bias. Then, unitary adjacency matrix is obtained with a unitary projection algorithm, which is implemented by utilizing the intrinsic structure of unitary adjacency matrix and allows GUMP to be permutation-equivariant. Experimental results show the effectiveness of GUMP in improving the performance on various graph learning tasks.

1. Introduction

Graph neural networks (GNNs) (Scarselli et al., 2008) have been widely used in various applications, such as social network (Fan et al., 2019) and knowledge graphs (Schlichtkrull et al., 2018). The most popular GNNs follow the message passing mechanism (Gilmer et al., 2017) to update the node representations, where each node aggregates feature vectors of its neighbors to compute its new feature vector. The message passing mechanism is designed to be permutation-equivariant, allowing GNNs to work with graphs that have varying node orders. Currently, GNNs with message passing mechanism have demonstrated success in various graph learning tasks, such as node classification (Kipf & Welling, 2016a), graph classification (Ying et al., 2018), and link prediction (Kipf & Welling, 2016b).

¹Department of Electronic Engineering, Tsinghua University, Beijing, China ²Tencent AI Lab, Shenzhen, China. Correspondence to: Quanming Yao <first1.last1@xxx.edu>.

Preprint. Under review.

However, the message passing mechanism also inevitably brings the oversquashing problem to GNNs (Alon & Yahav, 2020; Topping et al., 2022; Banerjee et al., 2022). The oversquashing problem draws inspiration from a similar phenomenon observed in RNNs when learning long-range sequences, as noted by Alon & Yahav (2020). It refers to the situation where, as larger neighborhoods are considered, information from distant interactions funneled through specific bottlenecks minimally influences GNN training. This phenomenon involves compressing information from potentially exponentially many nodes (with respect to the number of layers) into fixed-sized node vectors.

Various techniques are proposed to alleviate the oversquashing problem. Topping et al. (2022) propose the Jacobian of GNN to measure oversquashing, which motivates a rewiring method that increases the curvature of the edges in graph. Most works combat oversquashing via methods depending on the graph spectrum (i.e., the eigenvalue of the adjacency matrix). In these works, rewiring techniques increase the spectral gap by flipping edges (Banerjee et al., 2022), adding edges (Karhadkar et al., 2023), re-weighting the edges (Arnaiz-Rodríguez et al., 2022), or using expander for message passing (Deac et al., 2022). Except from increasing spectral gap, recent works bound the measure in Topping et al. (2022) with effective resistance (Black et al., 2023) and commute time (Di Giovanni et al., 2023), and propose rewiring techniques to improve these bounds. Except from improving graph spectrum, Barbero et al. (2023) propose rewiring method to greedily add edges to increase the number of walks in graph.

The rewiring techniques above, even motivated from different perspectives, can be justified from the Jacobian measure of oversquashing in Topping et al. (2022). For instance, increasing the spectral gap or effective resistance can be viewed as an indirect method of improving the entries of powers of the adjacency matrix in Jacobian measure. As a result, these rewiring methods have limited or uncertain improvements on Jacobian measure because some of them do not directly improve it (Karhadkar et al., 2023; Black et al., 2023) or improve it in a greedy way (Barbero et al., 2023). Moreover, the rewiring techniques disrupt the original graph structure, resulting in the loss of crucial structural biases in graph learning tasks (Battaglia et al., 2018). This makes the rewiring techniques inadequate for oversquashing.

In this paper, we propose Graph Unitary Message Passing (GUMP) to alleviate oversquashing. Motivated by existing analysis on oversquashing of RNNs (Pascanu et al., 2013; Jing et al., 2017), the measures of oversquashing in RNNs and GNNs share similar forms (Figure 1(a)), i.e., the powers of feature transformation matrix in RNN and the powers of adjacency matrix in GNN (Section 3.1). Since the unitary parameterization of transformation matrix is proved to be effective in capturing long-range interactions (Arjovsky et al., 2016) in RNN, we consider imposing unitarity to adjacency matrix in GNN for message passing. With unitary adjacency matrix, the Jacobian measure of oversquashing will not change exponentially, thereby alleviating oversquashing. Compared to existing rewiring methods (Table 1), GUMP paves a new way for alleviating oversquashing, which achieves optimal Jacobian measure and preserves the structural bias of graphs.

To design GUMP, we first propose a graph transformation algorithm in Section 3.2 to make a general graph have unitary adjacency matrix and preserve its structural bias at the same time. The transformation algorithm is based on the theory showing that unitary adjacency matrix exists for the line graph of Eulerian graph. Then, we propose an algorithm to calculate unitary adjacency matrix in Section 3.3. The algorithm is designed to allow GUMP to be permutation-equivariant and is implemented by utilizing the intrinsic structure of unitary adjacency matrix. Finally, we evaluate GUMP on several graph learning tasks in Section 4. In summary, our paper has the following contributions:

- GUMP alleviates oversquashing by applying unitary adjacency matrix for message passing. Compared with previous works, GUMP achieves the optimal Jacobian measure of oversquashing.
- GUMP maintains the structural bias with a graph transformation algorithm and preserves the permutation equivariance of message passing with unitary projection.
- Extensive results show the effectiveness of GUMP. Further analysis on the Jacobian measure also shows that GUMP can alleviate oversquashing.

Notations In this paper, we use bold uppercase letters \mathbf{X} to denote matrices, bold lowercase letters \mathbf{x} to denote vectors, and lowercase letters x to denote scalars. Given a matrix \mathbf{X} , the i -th row of matrix \mathbf{X} is denoted as \mathbf{x}_i and the entry of the i -th row and j -th column of matrix \mathbf{X} is denoted as \mathbf{X}_{ij} . The transpose and conjugate transpose of matrix \mathbf{X} is denoted as \mathbf{X}^\top and \mathbf{X}^\dagger , respectively. A graph with n nodes and e edges is denoted as $G = (V, E, \mathbf{X})$ where $V = \{1, 2, \dots, n\}$ is the node set, $E \subseteq V \times V$ is the edge set, and $\mathbf{X} \in \mathbb{R}^{n \times d}$ is the d -dimensional node feature matrix. For convenience, the operator $V[G]$ and $E[G]$ are used to

denote the node set and edge set of graph G respectively, i.e., $V[G] = V$ and $E[G] = E$. The adjacency matrix of graph G is denoted as $\tilde{\mathbf{A}}[G] \in \mathbb{R}^{n \times n}$ where $\tilde{\mathbf{A}}_{ij} = 1$ if $(i, j) \in E$ and $\tilde{\mathbf{A}}_{ij} = 0$ otherwise. The normalized adjacency matrix of graph G is denoted as $\hat{\mathbf{A}}[G] \in \mathbb{R}^{n \times n}$ where $\hat{\mathbf{A}}[G] = \mathbf{D}^{-1/2} \tilde{\mathbf{A}}[G] \mathbf{D}^{-1/2}$ and \mathbf{D} is the degree matrix of graph G . We also use matrix $\mathbf{A}[G] \in \mathbb{R}^{n \times n}$ to represent the adjacency in graph G , i.e., $\mathbf{A}_{ij} \neq 0$ if $(i, j) \in E$ and $\mathbf{A}_{ij} = 0$ otherwise. For convenience, the adjacency matrices above are denoted as $\tilde{\mathbf{A}}$, $\hat{\mathbf{A}}$, and \mathbf{A} respectively.

2. Related work

2.1. GNN and oversquashing

Graph neural network (GNN) (Kipf & Welling, 2016a; Gilmer et al., 2017) with L layers is a type of neural network that uses graph G and initial node features $\mathbf{H}^{(0)} = \mathbf{X}$ to learn node representations $\mathbf{H}^{(L)}$. The k -th layer of GNN updates node representation via the message-passing formula

$$\mathbf{h}_i^{(k)} = \delta(\mathbf{h}_i^{(k-1)}, \phi(\{\{\psi(\mathbf{h}_j^{(k-1)}), j \in \mathcal{N}(i)\}\})),$$

where δ , ϕ , and ψ are combination, aggregation, and message functions respectively, $\{\{\dots\}\}$ is a multiset, and $\mathcal{N}(i) = \{j | (i, j) \in E\}$.

Even GNN achieves success in various graph learning tasks, it suffers from the oversquashing problem. The oversquashing problem is first noted by Alon & Yahav (2020). Inspired by Xu et al. (2018b), Topping et al. (2022) proposes to measure oversquashing with the Jacobian between node features at different levels of a GNN. Based on the measure, Topping et al. (2022) propose rewiring method to increase the curvature of the edges in graph. Many works combat oversquashing by improving the spectral gap of graph. Banerjee et al. (2022) measure oversquashing via the spectral gap of graph, employing a rewiring algorithm based on expander graph construction and effective resistance for edge sampling. Karhadkar et al. (2023) introduce FoSR, a rewiring method that maximizing the first-order change in the spectral gap of graph. Arnaiz-Rodríguez et al. (2022) introduced a GNN comprising a parameter-free layer for learning commute time and a rewiring layer to optimize spectral gap according to network characteristics and task requirements. Except from improving spectral gap, Black et al. (2023) focus on minimizing total resistance between node pairs and introduce the Greedy Total Resistance (GTR) rewiring method for oversquashing. Di Giovanni et al. (2023) analyze oversquashing with commute time. Barbero et al. (2023) propose a rewiring method to sequentially increase the number of walks between two nodes and preserve the locality in the original graph.

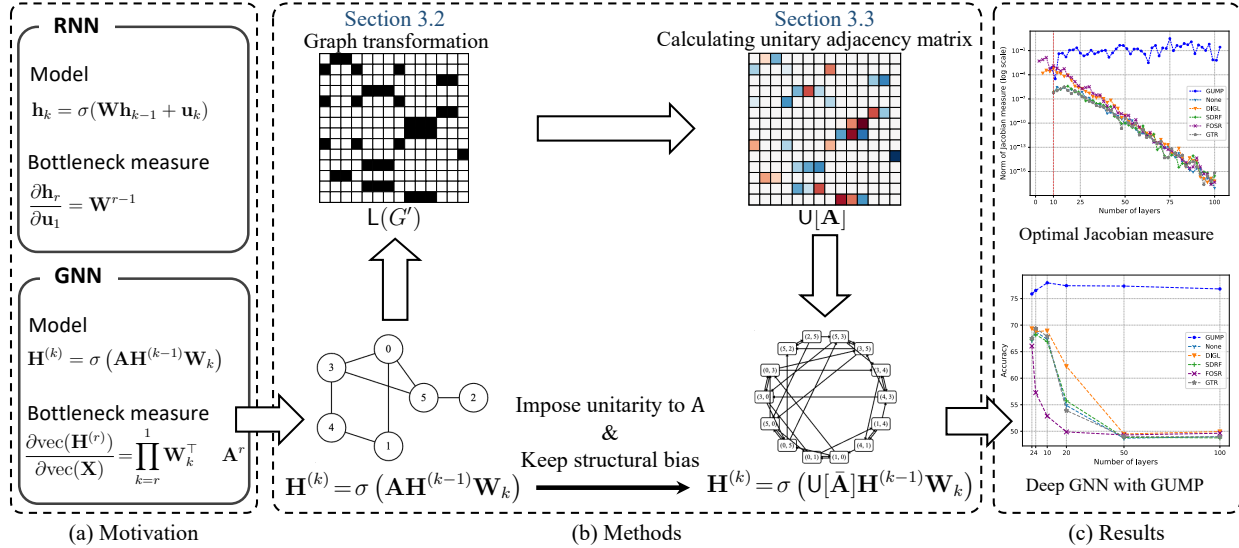


Figure 1. Overview of GUMP. (a) RNN versus GNN. The measures of bottleneck are derived with identity activation function and \otimes denotes Kronecker product. (b) GUMP aims to impose unitarity to \mathbf{A} while keeping structural bias of the original graph. GUMP achieves this goal with graph transformation (Section 3.2) and unitary adjacency matrix calculation (Section 3.3). (c) GUMP achieves the optimal Jacobian measure of oversquashing and its performance does not exhibit degradation when increasing the number of layers.

2.2. Unitary neural networks

Unitary matrices contribute to the stability of neural network training by preserving vector norms, preventing issues like exploding or vanishing gradients. Imposing unitarity on neural networks enhances their ability to seamlessly capture and propagate information across layers. This technique has proven successful in various architectures, such as RNNs, CNNs, and GNNs.

Unitary neural networks (UNNs) is first developed to tackle the problem of vanishing and exploding gradients in RNNs, enabling more efficient learning of information in extremely long sequences of data compared to existing methods like LSTM (Hochreiter & Schmidhuber, 1997). Early algorithms construct a series of parameterized unitary transformations to impose unitarity. EUNN (Jing et al., 2017) achieves this by composing layers of rotations, Fourier transforms, and other unitary transformations to parametrize unitary matrices. uRNN (Arjovsky et al., 2016) and scoRNN (Helfrich et al., 2018), on the other hand, maintain unitarity by performing a Cayley transformation to parametrize the full unitary space. expRNN (Lezcano-Casado & Martinez-Rubio, 2019), in contrast, parametrizes unitary matrices within the Lie algebra of the orthogonal/unitary group. projUNN (Kiani et al., 2022) first optimizes its parameters using gradient-based optimization and then maps the updated parameters to a unitary space.

Despite RNN, unitarity has also been applied to CNNs and GNNs. Unitary CNNs (Sedghi et al., 2018; Li et al., 2019; Singla & Feizi, 2021; Trockman & Kolter, 2021) introduce

various methods to restrict the convolutional filters to be unitary, e.g., via the Lie algebra of the orthogonal group (Singla & Feizi, 2021) and the Cayley transform (Trockman & Kolter, 2021). Ortho-GConv (Guo et al., 2022) imposes unitarity on the feature transformation matrix in GNNs.

3. The Proposed GUMP

3.1. Motivation

GUMP is motivated by the attempts in RNN in learning long sequences (Jing et al., 2017; Arjovsky et al., 2016). RNN and GNN face bottlenecks in learning sequences and graphs. The measure of these bottlenecks has been analyzed by Pascanu et al. (2013) for RNN and Topping et al. (2022) for GNN (i.e., oversquashing). Given the representations of a sequence $\mathbf{u}_1, \dots, \mathbf{u}_L$ and the initial node features of a graph as \mathbf{X} , the models and bottleneck measures of RNN and GNN are summarized in Figure 1(a).

From Figure 1(a), the bottlenecks of RNN and GNN can be attributed to the powers of feature transformation matrix and the powers of adjacency matrix, respectively. For instance, the adjacency matrix \mathbf{A} can be diagonalized as $\mathbf{A} = \mathbf{P}\mathbf{\Lambda}\mathbf{P}^{-1}$ where $\mathbf{\Lambda}$ is the diagonal matrix of eigenvalues. Then, the powers of adjacency matrix can be written as $\mathbf{A}^L = \mathbf{P}\mathbf{\Lambda}^L\mathbf{P}^{-1}$, containing an exponential term $\mathbf{\Lambda}^L$. Thus, the powers of matrix causes the bottleneck measure to have exponential dependence on the number of network layers in both RNN and GNN.

To alleviate such bottlenecks in RNN, imposing unitarity to

\mathbf{W} is proved to be effective to capture long-range interactions in sequences (Jing et al., 2017; Arjovsky et al., 2016). In this paper, motivated by unitary RNN, we propose GUMP to impose unitarity to \mathbf{A} in GNN to alleviate oversquashing. However, compared to unitary RNNs, there are two challenges to impose unitarity on \mathbf{A} . The first challenge is how to impose unitarity to \mathbf{A} while keeping the structural bias of the original graph, because adjacency matrix is sparse and almost all unitary matrices are dense. GUMP transforms the original graph to new graph which has unitary adjacency matrix and keeps structural bias in Section 3.2. The second challenge is how to obtain unitary adjacency matrix which depends on the input graph. GUMP utilizes unitary projection to calculate the unitary adjacency matrix while preserving permutation equivariance of message passing in Section 3.3. An overview of GUMP is shown in Figure 1.

3.2. Transformation of the original graph

We consider the general digraph instead of undirected graph to analyze the existence of unitary adjacency, while the undirected graph can be seen as a special digraph by splitting an undirected edge into two directed edges. We first formally define the unitary adjacency matrix as in Severini (2003). Given an adjacency matrix \mathbf{A} , its support matrix $\mathbf{S}[\mathbf{A}] \in \mathbb{R}^{n \times n}$ is a binary matrix with entries equal to one if the corresponding entry of \mathbf{A} is non-zero and equal to zero otherwise, i.e., $\mathbf{S}[\mathbf{A}]_{ij} = 1$, if $\mathbf{A}_{ij} \neq 0$ and $\mathbf{S}[\mathbf{A}]_{ij} = 0$, if $\mathbf{A}_{ij} = 0$. Then, the unitary adjacency matrix \mathbf{U}_G of graph G is a unitary matrix whose support is equal to the support of its adjacency matrix \mathbf{A} , i.e., $\mathbf{S}[\mathbf{U}_G] = \mathbf{S}[\mathbf{A}]$. Therefore, given a graph G , if there exists a unitary adjacency matrix \mathbf{U}_G , G is called the digraph of a unitary matrix.

Algorithm 1 Graph transformation

Require: A graph $G = (V, E)$;
 1: Initialize a new digraph $G' = (V, E')$;
 2: **for** $(i, j) \in E$ **do**
 3: Add (i, j) and (j, i) to E' ;
 4: **end for**
 5: Convert G' to its line graph $\mathbf{L}(G')$;
 6: **Return:** $\mathbf{L}(G')$.

We propose the transformation in Algorithm 1 for undirected graph G to make it have unitary adjacency matrix and preserve its structural bias. Algorithm 1 first transforms the undirected graph to be Eulerian graph G' (Definition B.2) by splitting each undirected edge into two directed edges. Then, it converts the Eulerian graph to its line graph $\mathbf{L}(G')$ (Definition B.1). Finally, $\mathbf{L}(G')$ has unitary adjacency matrix which is proved in the following proposition.

Proposition 3.1. *The line graph $\mathbf{L}(G')$ returned by Algorithm 1 is the digraph of a unitary matrix.*

Proposition 3.1 is proved in Appendix C. In Algorithm 1, the structural bias of the original graph is preserved because the splitting of undirected edge and the conversion to line graph do not introduce new connectivity between nodes that is absent in the original graph. Finally, Algorithm 1 takes as input graph G with n nodes and e edges, and outputs a line graph $\mathbf{L}(G')$ with $2e$ nodes.

3.3. Calculating unitary adjacency matrix

Because adjacency matrix are input-dependent, the unitary adjacency matrix need to be calculated for each graph. In this section, we propose an algorithm to calculate unitary adjacency matrix for GUMP.

3.3.1. PERMUTATION-EQUIVARIANT PROJECTION

Permutation equivariance of message passing is a key property for GNNs to work with graphs that have varying node orders. To achieve this, the calculation of unitary adjacency matrix has to be permutation equivariance. Our method consists of two steps: 1) calculate edge weights to form a weighted adjacency matrix; 2) impose unitarity to the weighted adjacency matrix.

Firstly, edge weight for $(i, j) \in E[\mathbf{L}(G')]$ is calculated with

$$\alpha_{ij} = \text{Tanh}(\mathbf{w}^\top \cdot \text{LeakyReLU}(\mathbf{W}_s \mathbf{h}_i + \mathbf{W}_t \mathbf{h}_j)) \quad (1)$$

where \mathbf{h}_i (\mathbf{h}_j) is the representations for node i (j) in $\mathbf{L}(G')$, $\mathbf{W}_s, \mathbf{W}_t \in \mathbb{R}^{d' \times d}$ are transformation matrices for source and target nodes of an edge respectively, and $\mathbf{w} \in \mathbb{R}^{d'}$ is a learnable parameters. Then, the weighted adjacency matrix of $\mathbf{L}(G')$, denoted as $\bar{\mathbf{A}} \in \mathbb{R}^{2e \times 2e}$, is formed from edge weights, i.e., $\bar{\mathbf{A}}_{ij} = \alpha_{ij}$.

After calculating $\bar{\mathbf{A}}$, we impose unitarity to $\bar{\mathbf{A}}$ by projection. We use the projection algorithm in Keller (1975), which takes advantage of the fact that the polar transformation yields the closest unitary matrix to a given matrix in terms of Frobenius norm. The following lemma describes the unitary projection in GUMP:

Lemma 3.2. *Given a weighted adjacency matrix $\bar{\mathbf{A}} \in \mathbb{R}^{2e \times 2e}$ of $\mathbf{L}(G')$, the unitary projection of $\bar{\mathbf{A}}$ is given by*

$$\mathbf{U}[\bar{\mathbf{A}}] := \arg \min_{\mathbf{U} \text{ is unitary}} \|\bar{\mathbf{A}} - \mathbf{U}\|_F^2 = \bar{\mathbf{A}} (\bar{\mathbf{A}}^\dagger \bar{\mathbf{A}})^{-\frac{1}{2}}. \quad (2)$$

Lemma 3.2 (proved in Appendix C) indicates that $\mathbf{U}[\bar{\mathbf{A}}] = \bar{\mathbf{A}} (\bar{\mathbf{A}}^\dagger \bar{\mathbf{A}})^{-\frac{1}{2}}$ is the unitary adjacency matrix for GUMP. Also, the unitary projection $\mathbf{U}[\bar{\mathbf{A}}]$ is guaranteed to be permutation-equivariant when $\bar{\mathbf{A}}$ is a full-rank matrix with the following proposition.

Proposition 3.3 (Strong permutation equivariance). *Given two permutation matrices \mathbf{P}_1 and \mathbf{P}_2 , if $\bar{\mathbf{A}}$ is a full-rank matrix, the unitary projection $\mathbf{U}[\bar{\mathbf{A}}]$ is equivariant to both*

row and column permutations of $\bar{\mathbf{A}}$, i.e., $\mathbf{P}_1 \mathbf{U}[\bar{\mathbf{A}}] \mathbf{P}_2^\top = \mathbf{U}[\mathbf{P}_1 \bar{\mathbf{A}} \mathbf{P}_2^\top]$.

By Proposition 3.3 (proved in Appendix C), the weighted adjacency matrix $\bar{\mathbf{A}}$ should be full-rank to guarantee permutation equivariance of GUMP. Empirically, (1), inspired by GATv2 (Brody et al., 2021), is full-rank in experiments and thus can guarantee the permutation equivariance of GUMP.

However, the unitary projection (2) is computationally expensive due to the inverse square root of $\bar{\mathbf{A}}^\dagger \bar{\mathbf{A}} \in \mathbb{R}^{2e \times 2e}$. In experiments, the unitary projection is computationally infeasible when the number of edges e or batch size is large.

3.3.2. FEASIBLE IMPLEMENTATION

By utilizing the intrinsic structure in unitary adjacency matrix, the feasible unitary projection is implemented in Algorithm 2. In Algorithm 2, weighted adjacency matrix $\bar{\mathbf{A}}$ is first calculated with (1) in step 1. Then, the intrinsic structure of $\bar{\mathbf{A}}$ allows it to be permuted to be block diagonal with permutation matrices \mathbf{P}_1 and \mathbf{P}_2 in line 2. The permuted diagonal matrix is denoted as $\mathbf{D} := \text{diag}(\mathbf{D}_1, \mathbf{D}_2, \dots, \mathbf{D}_b) = \mathbf{P}_1 \bar{\mathbf{A}} \mathbf{P}_2^\top$. By Proposition 3.3, the unitary projection of \mathbf{D} is equal to the matrix after applying row permutation \mathbf{P}_1 and column permutation \mathbf{P}_2 to $\mathbf{U}[\bar{\mathbf{A}}]$, i.e., $\mathbf{U}[\mathbf{P}_1 \bar{\mathbf{A}} \mathbf{P}_2^\top] = \mathbf{P}_1 \mathbf{U}[\bar{\mathbf{A}}] \mathbf{P}_2^\top$, indicating $\mathbf{U}[\bar{\mathbf{A}}] = \mathbf{P}_1^\top \mathbf{U}[\mathbf{P}_1 \bar{\mathbf{A}} \mathbf{P}_2^\top] \mathbf{P}_2$. Thus, $\mathbf{U}[\bar{\mathbf{A}}]$ can be efficiently calculated by first applying unitary projection to each block \mathbf{D}_i of \mathbf{D} in line 3 and then applying the inverse row and column permutation \mathbf{P}_1^\top and \mathbf{P}_2 to the unitary projection of \mathbf{D} in line 4. The correctness of Algorithm 2 is guaranteed in Proposition 3.4 (proved in Appendix C).

Proposition 3.4. *The matrix returned by Algorithm 2 for graph $L(G')$ is equal to $\bar{\mathbf{A}} (\bar{\mathbf{A}}^\dagger \bar{\mathbf{A}})^{-\frac{1}{2}}$.*

Algorithm 2 is computationally feasible from two perspectives. Firstly, it applies unitary projection (2) to block matrices \mathbf{D}_i , each with sizes d_1, d_2, \dots, d_b ($\sum_{i=1}^b d_i = 2e$). The computational complexity of Algorithm 2 is $\mathcal{O}(\sum_{i=1}^b d_i^3)$, in contrast to the complexity of $\mathcal{O}(8e^3)$ when applied to the large matrix $\bar{\mathbf{A}}$. This results in lower computational cost for unitarity projection of block diagonal matrices, particularly when the sizes of the block matrices are small. Secondly, the algorithm benefits from the existence of many block matrices \mathbf{D}_i with identical sizes because matrices of same size can be grouped and computed in parallel with PyTorch.

3.4. Complete algorithm

The complete algorithm (Algorithm 3) incorporates GUMP into GNN for graph learning tasks. Given a graph G , a base GNN first computes the initial node representations of G , i.e., $\mathbf{X}^{(0)} = \text{GNN}(\mathbf{X}, G)$. Then, Algorithm 1 transforms G to $L(G')$. The initial node repre-

Algorithm 2 Calculation of unitary adjacency matrix

Require: $L(G')$ outputted by Algorithm 1;

- 1: Calculate $\bar{\mathbf{A}}$ of $L(G')$ with (1);
 - 2: Find the permutation matrices $\mathbf{P}_1, \mathbf{P}_2$ such that $\mathbf{D} := \text{diag}(\mathbf{D}_1, \dots, \mathbf{D}_b) = \mathbf{P}_1 \bar{\mathbf{A}} \mathbf{P}_2^\top$ is block diagonal;
 - 3: Calculate $\mathbf{U}[\mathbf{D}] = \text{diag}(\mathbf{U}[\mathbf{D}_1], \mathbf{U}[\mathbf{D}_2], \dots, \mathbf{U}[\mathbf{D}_b])$;
 - 4: Calculate $\mathbf{U}[\bar{\mathbf{A}}] = \mathbf{P}_1^\top \mathbf{U}[\mathbf{D}] \mathbf{P}_2$;
 - 5: **Return:** Unitary adjacency matrix $\mathbf{U}[\bar{\mathbf{A}}]$.
-

sentations $\mathbf{H}^{(0)} \in \mathbb{R}^{2e \times 2d}$ of $L(G')$ is generated with $\mathbf{h}_{(i,j)} = [\mathbf{x}_i^{(0)}; \mathbf{x}_j^{(0)}], \forall (i, j) \in \mathcal{V}[L(G')]$ ($i, j \in \mathcal{V}[G]$). Next, the unitary adjacency matrix $\mathbf{U}[\bar{\mathbf{A}}]$ of $L(G')$ is calculated from Algorithm 2 and applied to propagate messages in graph with $\mathbf{H}^{(k)} = \sigma(\mathbf{U}[\bar{\mathbf{A}}] \mathbf{H}^{(k-1)} \mathbf{W}_r)$. After L layers of unitary message passing, we obtain the node representations $\mathbf{H}^{(L)}$, which is later scattered to nodes of G with $\mathbf{H}_s^{(L)} = \text{Scatter}(\mathbf{H}^{(L)}, G) \in \mathbb{R}^{n \times d'}$. Then, $\mathbf{H}_s^{(L)}$ are concatenated with $\mathbf{X}^{(0)}$ to obtain the final node representations $\mathbf{X}^{(L)} = [\mathbf{X}^{(0)}; \mathbf{H}_s^{(L)}] \in \mathbb{R}^{n \times (d+d')}$ of G . Finally, various graph learning tasks are performed based on $\mathbf{X}^{(L)}$.

Algorithm 3 Graph unitary message passing

Require: A graph $G = (V, E, \mathbf{X})$;

- 1: $\mathbf{X}^{(0)} = \text{GNN}(\mathbf{X}, G)$;
 - 2: Transform G to $L(G')$ with Algorithm 1;
 - 3: Generate initial representation $\mathbf{H}^{(0)}$ for $L(G')$ with $\mathbf{h}_{(i,j)} = [\mathbf{x}_i^{(0)}; \mathbf{x}_j^{(0)}], \forall (i, j) \in \mathcal{V}[L(G')]$;
 - 4: Calculate $\mathbf{U}[\bar{\mathbf{A}}]$ with Algorithm 2;
 - 5: **for** $k = 1 \dots L$ **do**
 - 6: $\mathbf{H}^{(k)} = \sigma(\mathbf{U}[\bar{\mathbf{A}}] \mathbf{H}^{(k-1)} \mathbf{W}_k)$
 - 7: **end for**
 - 8: Scatter $\mathbf{H}^{(L)}$ to nodes of G with $\mathbf{H}_s^{(L)} = \text{Scatter}(\mathbf{H}^{(L)}, G)$;
 - 9: Generate node representations of G with $\mathbf{X}^{(L)} = [\mathbf{X}^{(0)}; \mathbf{H}_s^{(L)}]$.
 - 10: **Return:** Node representations $\mathbf{X}^{(L)}$ of G .
-

We also provide a theoretical analysis of GUMP to show that GUMP can alleviate oversquashing. Our theory is based on GNN model from Figure 1(a) with activation function being ReLU. GUMP is analyzed with \mathbf{A} being unitary and classical message passing is analyzed with \mathbf{A} being the normalized adjacency matrix. Motivated by Xu et al. (2018b), we analyze with expected Jacobian measure.

Theorem 3.5 (GUMP). *The expected Jacobian measure for GUMP, i.e., \mathbf{A} is unitary in GNN, is approximately in the order of $\mathbb{E}[\partial \mathbf{h}_i^{(L)} / \partial \mathbf{x}_s] = \mathcal{O}(1)$.*

Since oversquashing is mainly caused by decay/explosion of Jacobian measure, Theorem 3.5 indicates that Jacobian measure of GUMP does not change exponentially with respect to L and thus alleviates oversquashing. Theorem 3.5 does

Table 1. Comparison of different methods for oversquashing on important properties of GNN and Jacobian measure. “Permutation equivariance” denotes the order of nodes in the graph does not affect the node representations of GNN. “Measure” represents the measure of oversquashing used in the corresponding method. “Jacobian measure w.r.t L ” denotes the order of the expected Jacobian measure with respect to the number of layers L (Theorems 3.5 and 3.6).

Methods	SDRF	FoSR	LASER	GTR	GUMP
Permutation equivariance	✓	✗	✓	✓	✓
Structural bias	✗	✗	✗	✗	✓
Measure	curvature	spectral gap	walks	effective resistance	Jacobian
Jacobian measure w.r.t L	$\mathcal{O}(c^L)$	$\mathcal{O}(c^L)$	$\mathcal{O}(c^L)$	$\mathcal{O}(c^L)$	$\mathcal{O}(1)$

not indicate the Jacobian measure of GUMP is independent of L . In fact, the relation between Jacobian measure and L is a trigonometric function in GUMP, which can be bounded by constants. Next theorem analyzes the expected Jacobian measure of classical message passing.

Theorem 3.6 (Classical message passing). *The expected Jacobian measure for classical message passing, i.e., $\mathbf{A} = \hat{\mathbf{A}}$ in GNN, is approximately in the order of $\mathbb{E}[\partial \mathbf{h}_i^{(L)} / \partial \mathbf{x}_s] = \mathcal{O}(c^L)$, where $c \in (0, 1)$.*

Theorem 3.6 shows that the Jacobian measure of classical message passing decays exponentially with respect to L , thus leading to oversquashing. Therefore, Theorems 3.5 and 3.6 indicate that GUMP can achieve optimal Jacobian measure of oversquashing, i.e., $\mathcal{O}(1)$, while the classical message passing cannot. Theorems 3.5 and 3.6 are validated by experiments in Section 4.3 and proved in Appendix C.

3.5. Comparison with existing methods

Compared with previous works for oversquashing, GUMP paves a new way to solve the oversquashing problem instead of rewiring. Overall, GUMP has the following advantages: (1) GUMP is permutation-equivariant, which is a desirable property for graph learning. (2) Unlike rewiring methods, GUMP does not introduce extra connectivity to the original graph and thus preserves the structural bias in graphs. (3) GUMP achieves optimal Jacobian measure of oversquashing since the eigenvalues of unitarity adjacency matrix are complex unit and thus will not change exponentially with respect to the number of GNN layers. The comparison of GUMP and other oversquashing methods are in Table 1.

Previous work on unitary GNN, e.g., Ortho-GConv (Guo et al., 2022), imposes unitarity on the feature transformation matrix of GNN. Unlike Ortho-GConv, GUMP addresses the issue of ill-posed gradient caused by oversquashing by imposing unitarity on adjacency matrix. Moreover, enforcing unitarity on adjacency matrix is more challenging than that on feature transformation, since adjacency matrix depends on input graph and is not parameter of GNN.

4. Experiments

In this section, we perform experiments to evaluate GUMP on graph learning tasks. All experiments are implemented by PyTorch Geometric (Fey & Lenssen, 2019) and conducted on NVIDIA RTX 4090 GPUs.

4.1. Experiments on the TUDataset

Datasets We select six datasets, i.e., Mutag, Proteins, Enzymes, IMDB-Binary, NCI1, and NCI109 from the TUDataset (Morris et al., 2020). Some datasets, e.g., REDDIT-BINARY, are not included in our experiments because there are too many edges per graph (e.g., more than 1000) in their datasets so that the unitary projection is computationally infeasible. The statistics of these datasets are in Table 4.

Baselines Baselines include DIGL (Gasteiger et al., 2019), SDRF (Topping et al., 2022), FoSR (Karhadkar et al., 2023), and GTR (Black et al., 2023). All baselines use GIN or GCN as base GNN for fair comparison. The baselines follows the settings of Karhadkar et al. (2023).

Experimental details To evaluate each method, we initially designate a test set comprising 10% of the graphs and a development set encompassing the remaining 90% of the graphs. The accuracies of each configuration are determined through 100 random train/validation splits of the development set, with 80% for training and 10% for validation. During the training phase, a stopping patience of 100 epochs is employed based on validation loss. Subsequently, for the test results, we report 95% confidence intervals for the best validation accuracy observed across the 100 runs.

In the experiments, the base GNN for GUMP is set to be GCN (Kipf & Welling, 2016a) and GIN (Xu et al., 2018a) for fair comparisons. The number of layers for base GNN is set to be in the range of one to five. Moreover, the number of layers for GUMP is manually tuned because the long-range interactions in graph can only be captured by increasing its layers. The detailed hyperparameters of GUMP for different datasets are presented in Table 5.

Table 2. Graph classification accuracy on the TUDataset. **First, second, and third** best results are colored for corresponding base GNNs.

Base GNN	Methods	Mutag	Proteins	Enzymes	IMDB-Binary	NCI1	NCI109	Rank
GCN	None	72.15±2.44	70.98±0.74	27.67±1.16	49.77±0.82	68.74±0.45	67.90±0.50	4.17
	None (+layer)	70.05±1.83	69.80±0.99	23.63±1.07	49.31±0.95	63.94±1.34	55.92±1.26	6.83
	DIGL	79.70±2.15	70.76±0.77	35.72±1.12	64.39±0.91	69.76±0.42	69.37±0.43	2.67
	SDRF	71.05±1.87	70.92±0.79	28.37±1.17	49.40±0.90	68.21±0.43	66.78±0.44	5.00
	FoSR	80.00±1.57	73.42±0.81	25.07±0.99	49.66±0.86	57.27±0.54	56.82±0.60	4.67
	GTR	79.10±1.86	72.59±2.48	27.52±0.99	49.92±0.99	69.37±0.38	67.97±0.47	3.50
	GUMP	84.89±1.63	74.88±0.87	36.02±1.43	60.00±1.24	77.97±0.42	75.85±0.44	1.17
GIN	None	77.70±3.60	70.80±0.83	33.80±1.12	70.18±0.99	75.65±0.49	74.93±0.46	4.00
	None (+layer)	69.80±2.75	68.71±0.96	25.92±1.07	69.61±1.26	73.49±0.46	72.47±0.53	6.50
	DIGL	79.80±2.08	70.71±0.67	35.74±1.20	64.43±0.89	79.37±0.43	76.88±0.39	3.50
	SDRF	78.40±2.80	69.81±0.79	35.82±1.09	69.72±1.15	74.55±0.54	73.89±0.43	4.33
	FoSR	78.00±2.22	75.11±0.82	29.20±1.38	71.21±0.92	70.15±0.47	69.93±0.45	4.67
	GTR	77.60±2.84	73.13±0.69	30.57±1.42	71.28±0.86	75.45±0.44	75.28±0.42	3.67
	GUMP	86.72±1.53	75.43±0.70	48.43±1.24	70.50±0.73	81.25±0.37	78.45±0.44	1.33

Results The results of GUMP on the TUDataset are shown in Table 2 with base GNN as GCN and GIN. Firstly, the results show that GUMP outperforms all baselines on all datasets except IMDB-Binary. Especially, GUMP outperforms baselines by a large margin on Mutag, Enzymes, NCI1, and NCI109. On IMDB-Binary, GUMP achieves comparable performance against FoSR and GTR in GIN while ranking second in GCN. Also, GUMP with base GNN as GIN achieves better performance than GUMP with base GNN as GCN on all datasets, which indicates that the representations of base GNN are crucial for GUMP since the unitary adjacency matrix are derived from these representations. Considering the average ranks of all baselines, DIGL has average rank of 2.67 in GCN and 3.50 in GIN, indicating it is unstable in different base GNNs. While for the rank of other baselines, their ranking is larger than 3, indicating their performance changes a lot in different datasets. Moreover, since GUMP usually has more layers than baselines in these datasets, the experiments shows that GCN and GIN with more layers has degraded performance on all datasets, showing that the improvement of GUMP does not come from increasing expressivity with more GNN layers.

4.2. Experiments on LRGB

In this section, we conduct experiments on the Long Range Graph Benchmark (LRGB) (Dwivedi et al., 2022), which is a set of GNN benchmarks involving long-range interactions. Following Barbero et al. (2023), three datasets are selected from LRGB, i.e., Peptides-func, Peptides-struct, and PCQM-contact. The statistics of these datasets are shown in Table 4.

The experiments of LRGB are conducted following the standard settings in Dwivedi et al. (2022). We set SDRF, FoSR, GTR, and LASER (Barbero et al., 2023) as baselines.

Table 3. Results of Peptides-func, Peptides-struct, and PCQM-contact with GCN. Best results are **bold**.

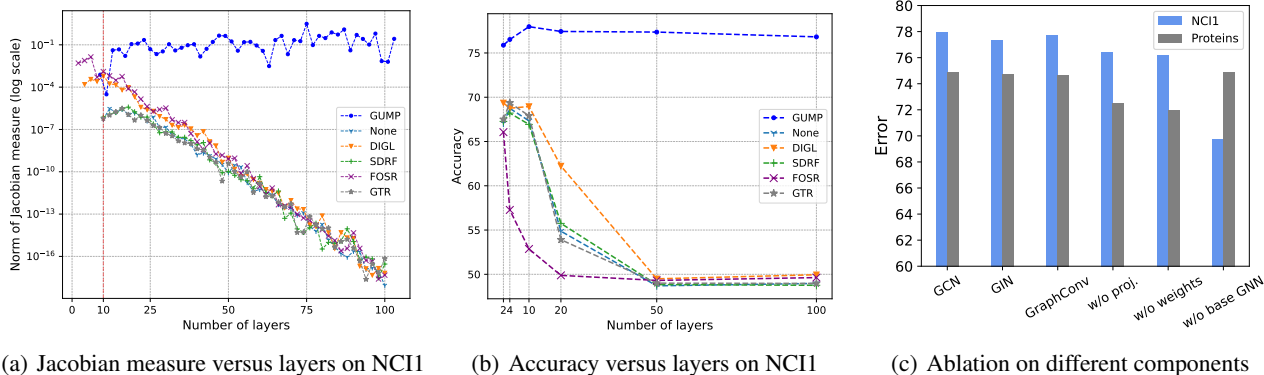
	Peptides-func Test AP \uparrow	Peptides-struct Test MAE \downarrow	PCQM-contact Test MRR \uparrow
None	.5930±.0023	.3496±.0013	.3234±.0006
SDRF	.5947±.0035	.3404±.0015	.3249±.0006
FoSR	.5947±.0027	.3078±.0026	.2783±.0008
GTR	.5075±.0029	.3618±.0010	.3007±.0022
LASER	.6440±.0010	.3043±.0019	.3275±.0011
GUMP	.6843±.0037	.2564±.0023	.3413±.0015

The hyperparameters of GUMP for LRGB are presented in Table 5. The results of LRGB are shown in Table 3. The results show that GUMP outperforms all baselines, which indicates that GUMP is more suitable for graph learning tasks involving long-range interactions than previous rewiring methods. The results of some rewiring methods, e.g., GTR, are worse than GCN, indicating that the greedy algorithm and measure used by it to alleviate oversquashing is not robust and may not help improve the performance of GNN in real applications.

4.3. Model analysis

In this section, we perform more experiments to analyze GUMP from three aspects, i.e., Jacobian measure, number of layers, and ablation studies.

We first visualize the Jacobian measure of oversquashing for GUMP and other baselines. We choose a pair of nodes with distance ten from NCI1 and calculate the spectral norm of Jacobian measure for GUMP and baselines with base GNN as GCN. The visualization is shown in Figure 2(a)



(a) Jacobian measure versus layers on NCI1 (b) Accuracy versus layers on NCI1 (c) Ablation on different components

Figure 2. Model analysis. GCN, GIN, and GUMP in (c) represent the convolution of GUMP. The base GNN of GUMP is GCN. “w/o proj” removes unitary projection in GUMP. “w/o weights” removes weighted adjacency matrix and unitary projection in GUMP. “w/o base GNN” removes base GNN in GUMP.

with norm of Jacobian measure in log scale. Firstly, when increasing the number of layers of GNNs, the Jacobian measure of GUMP does not decay, while the Jacobian measure of other baselines decays exponentially. The results validate the theoretical analysis in Theorems 3.5 and 3.6, indicating that GUMP has the ability to capture long-range interactions in graph without oversquashing. Secondly, the norm of Jacobian measure varies for different baselines. For example, DIGL has large norm of Jacobian measure when the number of layers is smaller than 50. Therefore, we can see that DIGL performs better than other baselines in Table 2. However, all these baselines has close norm of Jacobian measure when the number of layers is larger than 50.

Number of GNN layers indicates the ability of GNNs to capture long-range interactions. We further increase the number of layers of GUMP and baselines to see how their performances changes. This experiments is conducted in NCI1 with base GNN as GCN and set the number of layers in the range of 2 to 100. The other hyperparameters of GUMP are the same as Table 5. The results in Figure 2(b) demonstrate that the performance of GUMP increases from 75.88% to 77.97% when increasing the number of layers from 2 to 10. However, the performance of baselines decreases a lot when increasing the number of layers. For example, the performance of FoSR decreases from 66.06% to 52.86% when the number of layers increases from 2 to 10. The performance of baselines changes drastically as the layers increase, while the performance of GUMP are more stable. The results show GUMP can be deeper than previous methods, thus learning long-range interactions in graphs.

Lastly, we conduct ablation studies to analyze GUMP in Figure 2(c). We first replace the convolution of GUMP to GIN and GraphConv (Morris et al., 2019), showing that the choice of convolution has minor impact on the performance of GUMP. Then, we remove unitary projection (i.e., message passing with $\tilde{\mathbf{A}}$) and weighted adjacency matrix

(i.e., message passing with $\tilde{\mathbf{A}}[L(G')]$) in GUMP and the results show that their performances decrease, indicating the importance of GUMP. Finally, we remove the base GNN in GUMP and the results show that the performance of GUMP varies on different datasets, i.e., the performance on NCI1 decreases, while the performance on Proteins does not decrease. This phenomenon is expected because the quality of unitary adjacency matrix depends on the representations of nodes in the line graph (see (1)).

In model analysis, GUMP demonstrates the optimal Jacobian measure of oversquashing, greater stability with increased layers compared to prior methods, highlighting the critical role of its design in achieving superior performance.

5. Conclusion

In this paper, we propose a novel method for oversquashing, i.e., Graph Unitary Message Passing (GUMP). Motivated by unitary RNNs, GUMP propagates messages on graph with unitary adjacency matrix. Compared to previous methods, GUMP achieves optimal Jacobian measure of oversquashing, keeps the structural bias of the original graph, and is permutation-equivariant. In the future, we will try to improve the efficiency of GUMP and apply GUMP to more graph learning tasks.

Limitations and Impacts Our work may inspire future efforts to address the oversquashing problem by drawing insights from RNNs. As for limitations, unitary adjacency matrix requires many computational resources to calculate, which is infeasible for graphs with large number of edges. For weighted graph, since GUMP utilizes unitary adjacency matrix, the edge weights cannot be incorporated into message passing directly, and one possible way to resolve it is to convert edge weights to edge features similar to R-GNN (Battaglia et al., 2018).

Impact Statements

This paper presents work whose goal is to advance the field of Machine Learning. There are many potential societal consequences of our work, none which we feel must be specifically highlighted here.

References

- Alon, U. and Yahav, E. On the bottleneck of graph neural networks and its practical implications. *arXiv preprint arXiv:2006.05205*, 2020.
- Arjovsky, M., Shah, A., and Bengio, Y. Unitary evolution recurrent neural networks. In *International conference on machine learning*, pp. 1120–1128. PMLR, 2016.
- Arnaiz-Rodríguez, A., Begga, A., Escolano, F., and Oliver, N. M. Diffwire: Inductive graph rewiring via the lovász bound. In *The First Learning on Graphs Conference, 2022*. URL <https://openreview.net/forum?id=IXvfIex0mX6f>.
- Banerjee, P. K., Karhadkar, K., Wang, Y. G., Alon, U., and Montúfar, G. Oversquashing in gnns through the lens of information contraction and graph expansion. In *2022 58th Annual Allerton Conference on Communication, Control, and Computing (Allerton)*, pp. 1–8. IEEE, 2022.
- Bang-Jensen, J. and Gutin, G. Z. *Digraphs: theory, algorithms and applications*. Springer Science & Business Media, 2008.
- Barbero, F., Velingker, A., Saberi, A., Bronstein, M., and Di Giovanni, F. Locality-aware graph-rewiring in gnns. *arXiv preprint arXiv:2310.01668*, 2023.
- Battaglia, P. W., Hamrick, J. B., Bapst, V., Sanchez-Gonzalez, A., Zambaldi, V., Malinowski, M., Tacchetti, A., Raposo, D., Santoro, A., Faulkner, R., et al. Relational inductive biases, deep learning, and graph networks. *arXiv preprint arXiv:1806.01261*, 2018.
- Black, M., Wan, Z., Nayyeri, A., and Wang, Y. Understanding oversquashing in gnns through the lens of effective resistance. In *International Conference on Machine Learning*, pp. 2528–2547. PMLR, 2023.
- Brody, S., Alon, U., and Yahav, E. How attentive are graph attention networks? In *International Conference on Learning Representations*, 2021.
- Deac, A., Lackenby, M., and Veličković, P. Expander graph propagation. In *Learning on Graphs Conference*, pp. 38–1. PMLR, 2022.
- Di Giovanni, F., Giusti, L., Barbero, F., Luise, G., Lio, P., and Bronstein, M. M. On over-squashing in message passing neural networks: The impact of width, depth, and topology. In *International Conference on Machine Learning*, pp. 7865–7885. PMLR, 2023.
- Dwivedi, V. P., Rampásek, L., Galkin, M., Parviz, A., Wolf, G., Luu, A. T., and Beaini, D. Long range graph benchmark. *Advances in Neural Information Processing Systems*, 35:22326–22340, 2022.
- Fan, W., Ma, Y., Li, Q., He, Y., Zhao, E., Tang, J., and Yin, D. Graph neural networks for social recommendation. In *The world wide web conference*, pp. 417–426, 2019.
- Fey, M. and Lenssen, J. E. Fast graph representation learning with PyTorch Geometric. In *ICLR Workshop on Representation Learning on Graphs and Manifolds*, 2019.
- Gasteiger, J., Weissenberger, S., and Günnemann, S. Diffusion improves graph learning. *Advances in neural information processing systems*, 32, 2019.
- Gilmer, J., Schoenholz, S. S., Riley, P. F., Vinyals, O., and Dahl, G. E. Neural message passing for quantum chemistry. In *International conference on machine learning*, pp. 1263–1272. PMLR, 2017.
- Guo, K., Zhou, K., Hu, X., Li, Y., Chang, Y., and Wang, X. Orthogonal graph neural networks. In *Proceedings of the AAAI Conference on Artificial Intelligence*, volume 36, pp. 3996–4004, 2022.
- Helfrich, K., Willmott, D., and Ye, Q. Orthogonal recurrent neural networks with scaled cayley transform. In *International Conference on Machine Learning*, pp. 1969–1978. PMLR, 2018.
- Hochreiter, S. and Schmidhuber, J. Long short-term memory. *Neural Comput.*, 9(8):1735–1780, nov 1997. ISSN 0899-7667. doi: 10.1162/neco.1997.9.8.1735. URL <https://doi.org/10.1162/neco.1997.9.8.1735>.
- Jing, L., Shen, Y., Dubcek, T., Peurifoy, J., Skirlo, S., LeCun, Y., Tegmark, M., and Soljačić, M. Tunable efficient unitary neural networks (eunn) and their application to rnns. In *International Conference on Machine Learning*, pp. 1733–1741. PMLR, 2017.
- Karhadkar, K., Banerjee, P. K., and Montufar, G. FoSR: First-order spectral rewiring for addressing oversquashing in GNNs. In *The Eleventh International Conference on Learning Representations*, 2023. URL <https://openreview.net/forum?id=3YjQfCLdrzz>.
- Keller, J. B. Closest unitary, orthogonal and hermitian operators to a given operator. *Mathematics Magazine*, 48(4):192–197, 1975.

- Kiani, B., Balestrieri, R., LeCun, Y., and Lloyd, S. projunn: Efficient method for training deep networks with unitary matrices. *Advances in Neural Information Processing Systems*, 35:14448–14463, 2022.
- Kipf, T. N. and Welling, M. Semi-supervised classification with graph convolutional networks. *arXiv preprint arXiv:1609.02907*, 2016a.
- Kipf, T. N. and Welling, M. Variational graph auto-encoders. *arXiv preprint arXiv:1611.07308*, 2016b.
- Lezcano-Casado, M. and Martinez-Rubio, D. Cheap orthogonal constraints in neural networks: A simple parametrization of the orthogonal and unitary group. In *International Conference on Machine Learning*, pp. 3794–3803. PMLR, 2019.
- Li, Q., Haque, S., Anil, C., Lucas, J., Grosse, R. B., and Jacobsen, J.-H. Preventing gradient attenuation in lipschitz constrained convolutional networks. *Advances in neural information processing systems*, 32, 2019.
- Morris, C., Ritzert, M., Fey, M., Hamilton, W. L., Lenssen, J. E., Rattan, G., and Grohe, M. Weisfeiler and leman go neural: Higher-order graph neural networks. In *Proceedings of the AAAI conference on artificial intelligence*, volume 33, pp. 4602–4609, 2019.
- Morris, C., Kriege, N. M., Bause, F., Kersting, K., Mutzel, P., and Neumann, M. Tudataset: A collection of benchmark datasets for learning with graphs. In *ICML 2020 Workshop on Graph Representation Learning and Beyond (GRL+ 2020)*, 2020. URL www.graphlearning.io.
- Pascanu, R., Mikolov, T., and Bengio, Y. On the difficulty of training recurrent neural networks. In *International conference on machine learning*, pp. 1310–1318. Pmlr, 2013.
- Scarselli, F., Gori, M., Tsoi, A. C., Hagenbuchner, M., and Monfardini, G. The graph neural network model. *IEEE transactions on neural networks*, 20(1):61–80, 2008.
- Schlichtkrull, M., Kipf, T. N., Bloem, P., Van Den Berg, R., Titov, I., and Welling, M. Modeling relational data with graph convolutional networks. In *The Semantic Web: 15th International Conference, ESWC 2018, Heraklion, Crete, Greece, June 3–7, 2018, Proceedings 15*, pp. 593–607. Springer, 2018.
- Sedghi, H., Gupta, V., and Long, P. M. The singular values of convolutional layers. *arXiv preprint arXiv:1805.10408*, 2018.
- Severini, S. On the digraph of a unitary matrix. *SIAM Journal on Matrix Analysis and Applications*, 25(1):295–300, 2003.
- Singla, S. and Feizi, S. Skew orthogonal convolutions. In *International Conference on Machine Learning*, pp. 9756–9766. PMLR, 2021.
- Topping, J., Di Giovanni, F., Chamberlain, B. P., Dong, X., and Bronstein, M. M. Understanding over-squashing and bottlenecks on graphs via curvature. In *International Conference on Learning Representations*, 2022.
- Trockman, A. and Kolter, J. Z. Orthogonalizing convolutional layers with the cayley transform. *arXiv preprint arXiv:2104.07167*, 2021.
- Xu, K., Hu, W., Leskovec, J., and Jegelka, S. How powerful are graph neural networks? *arXiv preprint arXiv:1810.00826*, 2018a.
- Xu, K., Li, C., Tian, Y., Sonobe, T., Kawarabayashi, K.-i., and Jegelka, S. Representation learning on graphs with jumping knowledge networks. In *International conference on machine learning*, pp. 5453–5462. PMLR, 2018b.
- Ying, Z., You, J., Morris, C., Ren, X., Hamilton, W., and Leskovec, J. Hierarchical graph representation learning with differentiable pooling. *Advances in neural information processing systems*, 31, 2018.

A. The Illustrated GUMP

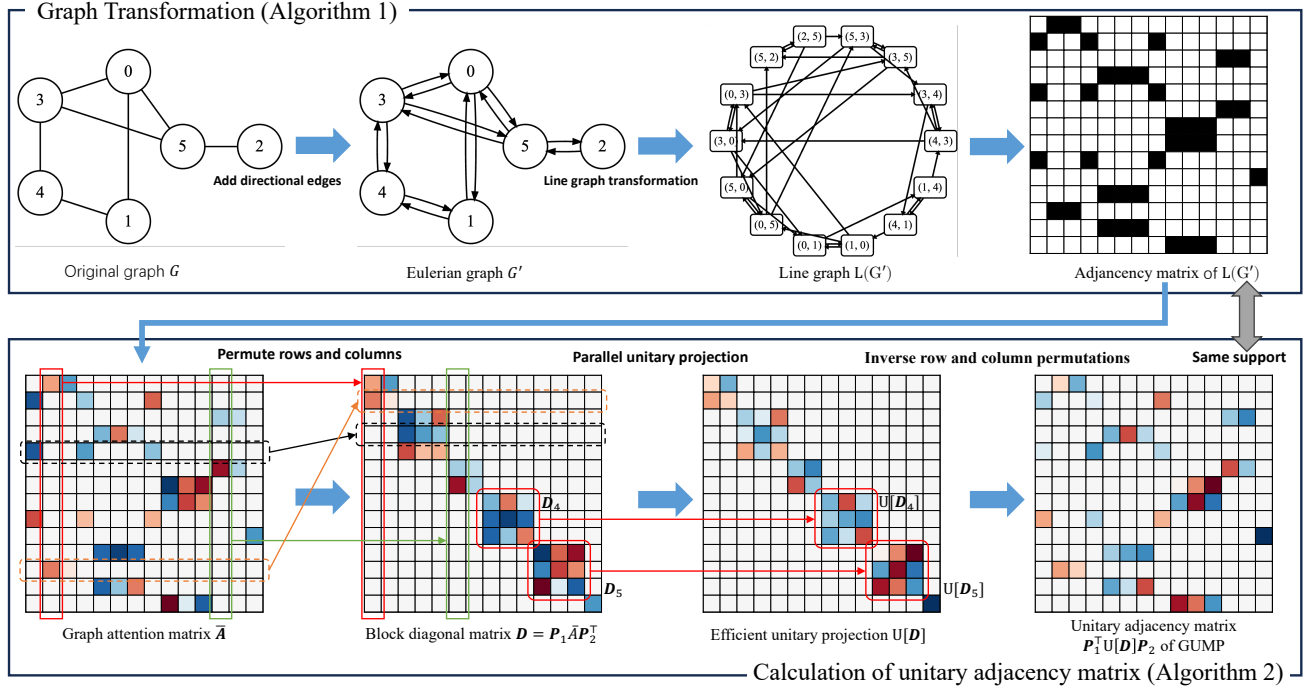


Figure 3. The illustrated GUMP.

B. Preliminaries

Definition B.1 (Line graph). Given a graph G , its line graph $L(G)$ is a graph such that

- each vertex of $L(G)$ represents an edge of G , i.e., $V[L(G)] = E[G]$;
- two vertices of $L(G)$ are adjacent if and only if their corresponding edges share a common endpoint in G , i.e., $E[L(G)] = \{(i, j), (j, k) \in V[L(G)] \times V[L(G)] \mid (i, j), (j, k) \in E[G]\}$.

Definition B.2 (Eulerian graph). An Eulerian graph G is a graph containing an Eulerian cycle, i.e., there is a trail in G that starts and ends on the same vertex and visits every edge exactly once.

Definition B.3 (Permutation matrix). A permutation matrix $\mathbf{P} \in \mathbb{R}^{n \times n}$ is a square binary matrix that has exactly one entry of 1 in each row and each column with all other entries 0.

Theorem B.4. Every permutation matrix is orthogonal, i.e., if \mathbf{P} is a permutation matrix, $\mathbf{P}^\top \mathbf{P} = \mathbf{P} \mathbf{P}^\top = \mathbf{I}$.

C. Proof

C.1. Proof of Proposition 3.1

Proposition 3.1 is proved based on the following theorem and lemma. Theorem C.1 is a direct result from Theorem 3 in Severini (2003). Lemma C.2 is a well known result in graph theory, which can be found in Theorem 1.7.2 of Bang-Jensen & Gutin (2008).

Theorem C.1 (Existence of unitary adjacency matrix). Let G be a single-connected digraph. Its line graph $L(G)$ (Definition B.1) is the digraph of a unitary matrix if and only if G is Eulerian (Definition B.2).

Lemma C.2 (A special Eulerian graph). A digraph graph is Eulerian if and only if it is connected and the in-degree and out-degree are equal at each vertex.

Proof of Proposition 3.1. In Algorithm 1, the undirected edges in G are split into two directed edges in G' . Therefore, the in-degree and out-degree of each vertex in G' are equal, indicating G' is Eulerian. Then, Theorem C.1 indicates that there exists unitary adjacency matrix \mathbf{U} such that $\mathbf{S}[\mathbf{U}] = \mathbf{A}[\mathbf{L}(G')]$. \square

C.2. Proof of Lemma 3.2

Proof. Given any unitary \mathbf{U} , let $\mathbf{U} = \mathbf{M} + \mathbf{U}[\bar{\mathbf{A}}]$ for the properly chosen $\mathbf{M} \in \mathbb{C}^{2e \times 2e}$. Due to the unitarity of \mathbf{U} and $\mathbf{U}[\bar{\mathbf{A}}]$, we have

$$\mathbf{M}\mathbf{U}[\bar{\mathbf{A}}]^\dagger + \mathbf{M}\mathbf{M}^\dagger + \mathbf{U}[\bar{\mathbf{A}}]\mathbf{M}^\dagger = 0. \quad (3)$$

Then, we have

$$\begin{aligned} \|\bar{\mathbf{A}} - \mathbf{U}\|_F^2 &= \|\bar{\mathbf{A}} - \mathbf{M} - \mathbf{U}[\bar{\mathbf{A}}]\|_F^2 \\ &= \|\bar{\mathbf{A}} - \mathbf{U}[\bar{\mathbf{A}}]\|_F^2 + \text{Tr}[\mathbf{M}\mathbf{U}[\bar{\mathbf{A}}]^\dagger + \mathbf{M}\mathbf{M}^\dagger + \mathbf{U}[\bar{\mathbf{A}}]\mathbf{M}^\dagger] - \text{Tr}[\mathbf{M}^\dagger\bar{\mathbf{A}} + \bar{\mathbf{A}}^\dagger\mathbf{M}] \\ &= \|\bar{\mathbf{A}} - \mathbf{U}[\bar{\mathbf{A}}]\|_F^2 - \text{Tr}[\mathbf{M}^\dagger\bar{\mathbf{A}} + \bar{\mathbf{A}}^\dagger\mathbf{M}] \\ &= \|\bar{\mathbf{A}} - \mathbf{U}[\bar{\mathbf{A}}]\|_F^2 - \text{Tr}[\mathbf{M}^\dagger\mathbf{U}[\bar{\mathbf{A}}](\bar{\mathbf{A}}^\dagger\bar{\mathbf{A}})^{\frac{1}{2}} + (\bar{\mathbf{A}}^\dagger\bar{\mathbf{A}})^{\frac{1}{2}}\mathbf{U}[\bar{\mathbf{A}}]^\dagger\mathbf{M}]. \end{aligned}$$

Then, from (3), we have $\mathbf{M}\mathbf{U}[\bar{\mathbf{A}}]^\dagger + \mathbf{U}[\bar{\mathbf{A}}]\mathbf{M}^\dagger = -\mathbf{M}\mathbf{M}^\dagger$,

$$\|\bar{\mathbf{A}} - \mathbf{U}\|_F^2 = \|\bar{\mathbf{A}} - \mathbf{U}[\bar{\mathbf{A}}]\|_F^2 + \text{Tr}[(\bar{\mathbf{A}}^\dagger\bar{\mathbf{A}})^{\frac{1}{2}}\mathbf{M}\mathbf{M}^\dagger]. \quad (4)$$

The second term above is non-negative because $\text{Tr}[(\bar{\mathbf{A}}^\dagger\bar{\mathbf{A}})^{\frac{1}{2}}\mathbf{M}\mathbf{M}^\dagger] = \text{Tr}[\mathbf{M}^\dagger(\bar{\mathbf{A}}^\dagger\bar{\mathbf{A}})^{\frac{1}{2}}\mathbf{M}]$ and $(\bar{\mathbf{A}}^\dagger\bar{\mathbf{A}})^{\frac{1}{2}}\mathbf{M}$ is positive semi-definite. Therefore, for all unitary \mathbf{U} ,

$$\|\bar{\mathbf{A}} - \mathbf{U}\|_F^2 \geq \|\bar{\mathbf{A}} - \mathbf{U}[\bar{\mathbf{A}}]\|_F^2. \quad (5)$$

The result is proved. \square

C.3. Proof of Proposition 3.3

Lemma C.3. For any unitary matrix \mathbf{U} , given two permutation matrices \mathbf{P}_1 and \mathbf{P}_2 , $\mathbf{P}_1\mathbf{U}\mathbf{P}_2^\top$ is also unitary.

Proof. Let $\hat{\mathbf{U}} = \mathbf{P}_1\mathbf{U}\mathbf{P}_2^\top$. Then, we have

$$\begin{aligned} \hat{\mathbf{U}}\hat{\mathbf{U}}^\dagger &= \mathbf{P}_1\mathbf{U}\mathbf{P}_2^\top\mathbf{P}_2\mathbf{U}^\dagger\mathbf{P}_1^\top = \mathbf{P}_1\mathbf{U}\mathbf{U}^\dagger\mathbf{P}_1^\top = \mathbf{P}_1\mathbf{P}_1^\top = \mathbf{I}, \\ \hat{\mathbf{U}}^\dagger\hat{\mathbf{U}} &= \mathbf{P}_2\mathbf{U}^\dagger\mathbf{P}_1^\top\mathbf{P}_1\mathbf{U}\mathbf{P}_2^\top = \mathbf{P}_2\mathbf{U}^\dagger\mathbf{U}\mathbf{P}_2^\top = \mathbf{P}_2\mathbf{P}_2^\top = \mathbf{I} \end{aligned}$$

which proves $\mathbf{P}_1\mathbf{U}\mathbf{P}_2^\top$ is unitary. \square

Proof of Proposition 3.3. This proposition is proved by the uniqueness of the unitary matrix $\mathbf{U}[\bar{\mathbf{A}}]$ when $\bar{\mathbf{A}}$ is a full-rank matrix.

Assume there exists another unitary matrix $\mathbf{U} = \mathbf{M} + \mathbf{U}[\bar{\mathbf{A}}]$ such that

$$\mathbf{U} = \arg \min_{\mathbf{U} \text{ is unitary}} \|\bar{\mathbf{A}} - \mathbf{U}\|_F^2. \quad (6)$$

According to the proof of Lemma 3.2, we have

$$\|\bar{\mathbf{A}} - \mathbf{U}\|_F^2 = \|\bar{\mathbf{A}} - \mathbf{U}[\bar{\mathbf{A}}]\|_F^2 + \text{Tr}[(\bar{\mathbf{A}}^\dagger\bar{\mathbf{A}})^{\frac{1}{2}}\mathbf{M}\mathbf{M}^\dagger].$$

Since $\bar{\mathbf{A}}$ is full-rank matrix, $(\bar{\mathbf{A}}^\dagger\bar{\mathbf{A}})^{\frac{1}{2}}$ is position definite. Therefore, we have

$$\|\bar{\mathbf{A}} - \mathbf{U}\|_F^2 > \|\bar{\mathbf{A}} - \mathbf{U}[\bar{\mathbf{A}}]\|_F^2. \quad (7)$$

which contradicts the assumption that \mathbf{U} is the minimizer of $\|\bar{\mathbf{A}} - \mathbf{U}\|_F^2$. Thus, the unitary projection of $\bar{\mathbf{A}}$ is unique when $\bar{\mathbf{A}}$ is full-rank.

Because $U[\bar{\mathbf{A}}]$ is unique and is the minimizer of $\|\bar{\mathbf{A}} - \mathbf{U}\|_F^2$, from Lemma C.3, we have $\mathbf{P}_1 U[\bar{\mathbf{A}}] \mathbf{P}_2^\top$ the minimizer of

$$\arg \min_{\mathbf{U} \text{ is unitary}} \|\mathbf{P}_1 \bar{\mathbf{A}} \mathbf{P}_2^\top - \mathbf{U}\|_F^2$$

for any permutation matrices \mathbf{P}_1 and \mathbf{P}_2 . Because $\mathbf{P}_1 \bar{\mathbf{A}} \mathbf{P}_2^\top$ is also full-rank, $\mathbf{P}_1 U[\bar{\mathbf{A}}] \mathbf{P}_2^\top$ is the unitary projection of $\mathbf{P}_1 \bar{\mathbf{A}} \mathbf{P}_2^\top$, which proves that $U[\mathbf{P}_1 \bar{\mathbf{A}} \mathbf{P}_2^\top] = \mathbf{P}_1 U[\bar{\mathbf{A}}] \mathbf{P}_2^\top$ for any permutation matrices \mathbf{P}_1 and \mathbf{P}_2 . \square

C.4. Proof of Proposition 3.4

We need the following lemma to prove Proposition 3.4.

Lemma C.4. *Given the adjacency matrix $\mathbf{A}[L(G')]$, its rows and columns can be permuted to transform $\mathbf{A}[L(G')]$ to be block diagonal.*

Proof. According to Theorem 2 in Severini (2003), since $L(G')$ is line graph, $L(G')$ is specular. By Lemma 1 in Severini (2003), since $L(G')$ is the digraph of a unitary matrix, $L(G')$ is strongly quadrangular. Then, by Theorem 1 in Severini (2003), since $L(G')$ is specular and strongly quadrangular, $\mathbf{A}[L(G')]$ is composed of independent matrices, thus its rows and columns can be permuted to transform $\mathbf{A}[L(G')]$ to be block diagonal. \square

Proof of Proposition 3.4. This proposition is proved by the following step by step analysis.

1. By Lemma C.4, we can permute the rows and columns of $\mathbf{A}[L(G')]$ to transform $\mathbf{A}[L(G')]$ to be block diagonal, i.e., $\mathbf{D} := \text{diag}(\mathbf{D}_1, \dots, \mathbf{D}_b) = \mathbf{P}_1 \mathbf{A}[L(G')] \mathbf{P}_2^\top$ is block diagonal, where \mathbf{P}_1 and \mathbf{P}_2 are permutation matrices.
2. Since $\bar{\mathbf{A}}$ is full-rank, by Proposition 3.3, the unitary projection of \mathbf{D} is equal to the matrix after applying row permutation \mathbf{P}_1 and column permutation \mathbf{P}_2 to $U[\bar{\mathbf{A}}]$, i.e., $U[\mathbf{P}_1 \bar{\mathbf{A}} \mathbf{P}_2^\top] = \mathbf{P}_1 U[\bar{\mathbf{A}}] \mathbf{P}_2^\top$. Using the property of permutation matrix (Theorem B.4), we have $U[\bar{\mathbf{A}}] = \mathbf{P}_1^\top U[\mathbf{P}_1 \bar{\mathbf{A}} \mathbf{P}_2^\top] \mathbf{P}_2$.
3. Finally, we have

$$\begin{aligned} U[\bar{\mathbf{A}}] &= \mathbf{P}_1^\top U[\mathbf{P}_1 \bar{\mathbf{A}} \mathbf{P}_2^\top] \mathbf{P}_2 \\ &= \mathbf{P}_1^\top U[\mathbf{D}] \mathbf{P}_2 \\ &= \mathbf{P}_1^\top \text{diag}(U[\mathbf{D}_1], \dots, U[\mathbf{D}_b]) \mathbf{P}_2, \end{aligned}$$

which proves the correctness of Algorithm 2. \square

C.5. Proof of Theorem 3.5

Motivated by Xu et al. (2018b), we first introduce the expected Jacobian measure of oversquashing.

Theorem C.5. *Given a L -layer GNN with ReLU as activation function, i.e., $\mathbf{H}^{(k)} = \text{ReLU}(\mathbf{A}\mathbf{H}^{(k-1)}\mathbf{W}_k)$, $\mathbf{H}^{(0)} = \mathbf{X}$, $k = 1 \dots L$, assume that all paths in the computation graph of the model are activated with the same probability of success ρ , the expected Jacobian measure of oversquashing is*

$$\mathbb{E} \left[\frac{\partial \mathbf{h}_i^{(L)}}{\partial \mathbf{x}_s} \right] = \rho \prod_{l=L}^1 \mathbf{W}_l^\top (\mathbf{A}^L)_{is}, \quad (8)$$

Proof. Denote by $\mathbf{f}_i^{(l)}$ the pre-activated feature of $\mathbf{h}_i^{(l)}$, i.e., $\mathbf{f}_i^{(l)} = \sum_{z \in \mathcal{N}^{(i)}} \mathbf{A}_{iz} \mathbf{h}_z^{(l-1)} \mathbf{W}_l$, for any $l = 1 \dots L$, we have

$$\frac{\partial \mathbf{h}_i^{(l)}}{\partial \mathbf{h}_s^{(0)}} = \text{diag} \left(\mathbf{1}_{\mathbf{f}_i^{(l)} > 0} \right) \cdot \left(\sum_{z \in \mathcal{N}^{(i)}} \mathbf{A}_{iz} \frac{\partial \mathbf{h}_z^{(l-1)}}{\partial \mathbf{h}_s^{(0)}} \right) \cdot \mathbf{W}_l^\top.$$

By chain rule, we get

$$\begin{aligned} \frac{\partial \mathbf{h}_i^{(L)}}{\partial \mathbf{h}_s^{(0)}} &= \sum_{p=1}^{\Psi} \left[\frac{\partial \mathbf{h}_i^{(L)}}{\partial \mathbf{h}_s^{(0)}} \right]_p \\ &= \sum_{p=1}^{\Psi} \prod_{l=L}^1 \text{diag} \left(\mathbf{1}_{\mathbf{f}_{v_p^l}^{(l)} > 0} \right) \mathbf{A}_{v_p^l v_p^{l-1}} \mathbf{W}_l^\top. \end{aligned}$$

Here, Ψ is the total number of paths $v_p^L v_p^{L-1} \dots v_p^1 v_p^0$ of length $L + 1$ from $v_p^0 = s$ to $v_p^L = i$. For $l = 1 \dots L - 1$, $v_p^{l-1} \in \mathcal{N}(v_p^l)$.

For each path p , the derivative $[\partial \mathbf{h}_i^{(L)} / \partial \mathbf{h}_s^{(0)}]_p$ represents a directed acyclic computation graph. At a layer l , we can express an entry of the derivative as

$$\left[\frac{\partial \mathbf{h}_i^{(L)}}{\partial \mathbf{h}_s^{(0)}} \right]_p^{(m,n)} = \prod_{l=L}^1 \mathbf{A}_{v_p^l v_p^{l-1}} \sum_{q=1}^{\Phi} Z_q \prod_{l=L}^1 w_q^{(l)},$$

where Φ is the number of paths q from the input neurons to the output neuron (m, n) , in the computation graph of $[\partial \mathbf{h}_i^{(L)} / \partial \mathbf{h}_s^{(0)}]_p$. For each layer l , $w_q^{(l)}$ is the entry of \mathbf{W}_l^\top that is used in the q -th path. Finally, $Z_q \in \{0, 1\}$ represents whether the q -th path is active ($Z_q = 1$) or not ($Z_q = 0$) as a result of ReLU activation of the entries of $\mathbf{f}_{v_p^l}^{(l)}$'s on the q -th path.

Under the assumption that Z_q is a Bernoulli random variable with success probability ρ . Because of $\mathbb{P}[Z_q = 1] = \rho, \forall q$, we have

$$\mathbb{E} \left[\left[\frac{\partial \mathbf{h}_i^{(L)}}{\partial \mathbf{h}_s^{(0)}} \right]_p^{(m,n)} \right] = \rho \prod_{l=L}^1 \mathbf{A}_{v_p^l v_p^{l-1}} \sum_{q=1}^{\Phi} \prod_{l=L}^1 w_q^{(l)}.$$

Then, the expected Jacobian measure of oversquashing is

$$\mathbb{E} \left[\frac{\partial \mathbf{h}_i^{(L)}}{\partial \mathbf{x}_s} \right] = \sum_{p=1}^{\Psi} \mathbb{E} \left[\left[\frac{\partial \mathbf{h}_i^{(L)}}{\partial \mathbf{h}_s^{(0)}} \right]_p \right] = \rho \prod_{l=L}^1 \mathbf{W}_l^\top (\mathbf{A}^L)_{is}.$$

□

Proof of Theorem 3.5. We analyze different components in the expected Jacobian measure (8).

Firstly, $\prod_{l=L}^1 \mathbf{W}_l^\top$ is the product of weight matrices in GNNs, which will not change exponentially with respect to L because the weight matrices are appropriately initialized to avoid exploding or decay.

Then, we focus the analysis on \mathbf{A}^L . We first diagonalize \mathbf{A} in complex space, i.e., $\mathbf{A} = \mathbf{P}\mathbf{\Lambda}\mathbf{P}^{-1}$ with $\mathbf{\Lambda}$ being a diagonal matrix with its diagonal elements being eigenvalues of \mathbf{A} . Since \mathbf{A} is unitary, the elements in $\mathbf{\Lambda}$ are complex units, i.e., $\mathbf{\Lambda} = \text{diag}(e^{i\theta_1}, e^{i\theta_2}, \dots, e^{i\theta_{2e}})$. Therefore, \mathbf{A}^L is equal to $\mathbf{P}\mathbf{\Lambda}^L\mathbf{P}^{-1}$, where $\mathbf{\Lambda}^L = \text{diag}(e^{i\theta_1 L}, e^{i\theta_2 L}, \dots, e^{i\theta_{2e} L})$ which is also a diagonal matrix with its diagonal elements being complex units. Then, we have $(\mathbf{A}^L)_{is} = \mathbf{P}_i \text{diag}(e^{i\theta_1 L}, e^{i\theta_2 L}, \dots, e^{i\theta_{2e} L}) (\mathbf{P}^{-1})_s$, which is a value that does not change exponentially with respect to L and can be bounded by constants. With Euler's formula, i.e., $e^{ix} = \cos x + i \sin x$, the relation between $(\mathbf{A}^L)_{is}$ and L is a trigonometric function.

Since trigonometric function can be bounded by constants, we have $\prod_{l=L}^1 \mathbf{W}_l^\top (\mathbf{A}^L)_{is}$ is bounded by constants, i.e., $\mathbb{E}[\partial \mathbf{h}_i^{(L)} / \partial \mathbf{x}_s] = \mathcal{O}(1)$. □

C.6. Proof of Theorem 3.6

Proof. We analyze the different components in the expected Jacobian measure (8).

Firstly, $\prod_{l=L}^1 \mathbf{W}_l^\top$ is the product of weight matrices in GNNs, which will not change exponentially with respect to L because the weight matrices are appropriately initialized to avoid exploding or decay.

Then, we focus the analysis on \mathbf{A}^L . We first diagonalize \mathbf{A} in complex space, i.e., $\mathbf{A} = \mathbf{P}\mathbf{\Lambda}\mathbf{P}^{-1}$ with $\mathbf{\Lambda}$ being a diagonal matrix with its diagonal elements being eigenvalues of \mathbf{A} . Since $\mathbf{A} = \hat{\mathbf{A}}$, the elements in $\mathbf{\Lambda}$ are in the range of 0 and 1, i.e., $\mathbf{\Lambda} = \text{diag}(\theta_1, \theta_2, \dots, \theta_{2e}), \theta_i \in [0, 1]$. Therefore, \mathbf{A}^L is equal to $\mathbf{P}\mathbf{\Lambda}^L\mathbf{P}^{-1}$, where $\mathbf{\Lambda} = \text{diag}(\theta_1^L, \theta_2^L, \dots, \theta_{2e}^L)$. Without any assumption on the graph structure, there are many eigenvalues smaller than one. Then, we have $(\mathbf{A}^L)_{is} = \mathbf{P}_i \text{diag}(\theta_1^L, \theta_2^L, \dots, \theta_{2e}^L) (\mathbf{P}^{-1})_s$, which is a value that change exponentially with respect to L .

Finally, we have $\prod_{l=L}^1 \mathbf{W}_l^\top (\mathbf{A}^L)_{is}$ in the order of $\mathcal{O}(c^L)$, i.e., $\mathbb{E}[\partial \mathbf{h}_i^{(L)} / \partial \mathbf{x}_s] = \mathcal{O}(c^L), c \in (0, 1)$. □

D. Detailed experiments

Table 4. Statistics of datasets.

	#graphs	Avg. nodes	Avg. edges	Task type
Mutag	188	17.9	39.6	Graph Classification
Proteins	1,113	39.1	145.6	Graph Classification
Enzymes	600	32.6	124.3	Graph Classification
IMDB-Binary	1,000	19.8	193.1	Graph Classification
NC1	4110	29.87	32.30	Graph Classification
NC109	4127	29.68	32.13	Graph Classification
Peptides-func	15,535	150.94	307.30	Graph Classification
Peptides-struct	15,535	150.94	307.30	Graph Regression
PCQM-contact	529,434	30.14	61.09	Link Prediction

Table 5. Hyperparameters of GUMP for datasets in experiments. $\text{layer}_{\text{GUMP}}$, lr_{base} , wd_{base} , lr_{GUMP} , wd_{GUMP} , drop. , d' , d , batch size, $\text{layer}_{\text{base}}$, opt. , sched. , and epoch denotes the number of layers of GUMP, learning rate of base GNN, weight decay of base GNN, learning rate of GUMP, weight decay of GUMP, dropout rate, dimension of calculating (1), hidden dimension of GNN, batch size, number of layers of base GNN, optimizer, scheduler, and number of epochs, respectively.

	$\text{layer}_{\text{GUMP}}$	lr_{base}	wd_{base}	lr_{GUMP}	wd_{GUMP}	drop.	d'	d	batch size	$\text{layer}_{\text{base}}$	opt.	sched.	epoch
Mutag	16	10^{-2}	10^{-4}	10^{-4}	0	0	32	64	16	5	adam	none	100
Proteins	20	10^{-2}	10^{-2}	10^{-4}	10^{-2}	0	32	64	64	3	adam	none	100
Enzymes	10	10^{-2}	10^{-4}	10^{-4}	0	0	32	64	16	1	adam	none	100
IMDB-Binary	24	10^{-2}	10^{-4}	10^{-4}	0	0	32	64	16	1	adam	none	100
NC1	10	10^{-2}	10^{-4}	10^{-4}	0	0	32	64	16	1	adam	none	100
NC109	10	10^{-2}	10^{-4}	10^{-4}	0	0	32	64	16	1	adam	none	100
Peptides-func	12	0.005	0.1	0.1	0.1	0.2	32	256	200	3	adam	cos.	250
Peptides-struct	12	0.005	0.1	0.005	0.1	0.2	32	256	200	3	adam	cos.	250
PCQM-contact	10	0.001	0	0.001	0	0.1	32	256	300	3	adam	cos.	150